Catalysis Communications 177 (2023) 106649

Contents lists available at ScienceDirect

Catalysis Communications

journal homepage: www.elsevier.com/locate/catcom

Furfural conversion over calcined Ti and Fe metal-organic frameworks under continuous flow conditions

Janejira Ratthiwal [a,b], Noelia Lazaro [a], Antonio Pineda [a], Roberto Esposito [a,c], Zeid A. ALOthman [d], Prasert Reubroycharoen [b], Rafael Luque [a,e,*]

[a] Departamento de Química Orgánica Universidad de Córdoba, Edificio Marie Curie (C 3), Campus de Rabanales, Ctra Nnal IV-A, Km 396, E14014 Córdoba, Spain
[b] Program in Petrochemistry and Polymer Science, Faculty of Science and Department of Chemical Technology, Faculty of Science, Chulalongkorn University, 254 Phayathai Road, Wangmai, Pathumwan, Bangkok 10330, Thailand
[c] Dipartimento di Scienze Chimiche, Università degli Studi di Napoli Federico II, Via Cintia-Complesso di Monte S. Angelo, 80126 Napoli, Italy
[d] Chemistry Department, College of Science, King Saud University, P.O. Box 2455, Riyadh, 11451, Saudi Arabia
[e] Universidad ECOTEC, Km. 13.5 Samborondón, Samborondón, EC092302, Ecuador

ARTICLE INFO

Keywords:
MIL-101(Fe)
MIL-125(Ti)
Furfural hydrogenation
Solvothermal method
Furfuryl alcohol

ABSTRACT

Furfural is an interesting bio-platform derived from lignocellulosic biomass that can be converted into chemicals and add-value products. In this work, the continuous-flow hydrogenation of furfural with 2-propanol was carried out using transition metal-based catalysts. C-MIL-101(Fe) and C-MIL-125(Ti), were successfully synthesized upon calcination of the parent MOFs obtained by the solvothermal method and their performances were compared in the hydrogenation of furfural. Interestingly, an 83% furfural conversion has been achieved over calcined C-MIL-125(Ti) with 77% of selectivity for FOL. Calcined C-MIL-101(Fe) provided lower furfural conversion and FOL selectivity, with an interesting switch towards acetal products.

1. Introduction

Biomass has been getting attention to use as a source of energy for a long time, especially in these decades due to the disadvantages of fossil fuels such as coal, natural gas, and petroleum oil. The utilization of non-renewable hydrocarbons causes air pollution and the greenhouse effect continuously. Thus, biomass from agriculture (sugarcane, cotton, wood, bagasse, corn) is an alternative option to replace or reduce using of fossil resources or produce some chemicals efficiently. Furfural (FF) is a product derived from the dehydration of xylose from lignocellulosic biomass enriched with pentose derivatives and it is an important starting material for the production of furfuryl alcohol (FOL), 2-methylfuran (2-MF), maleic acid, tetrahydrofuran (THF), levulinic acid (LA) and other useful chemicals [1–3]. Furfural production was established at industrial scale in 1921 [4]. In the last years, furfural production increased to 200,000 tons a year [5,6]. This makes it a very appetible renewable chemical platform that can be converted in many interesting products (Scheme 1). For example, furan and furoic acid can be obtained through decarboxylation and oxidation, respectively [7] while conversion to 5-hydroxymethylfuran (5-HMF) from hydrolysis of glucose (biomass) was also reported [8]. Furfural can also be transformed into levulinic acid which can be used as biofuel, fuel additive or other useful products [7,9,10]. Moreover, reductive amination and decarbonylation of furfural can produce furfurylamine and 2-methylfuran, respectively [7].

Ca. 62% of the furfural manufacture is converted to FOL. Generally, FOL is a starting material used in many industries to produce lubricants, plasticizers, vitamin C, adhesives, coatings, and resins [11,12]. In addition, FOL is an intermediate to synthesize 2-MF which is used as a gasoline blend or as an intermediate in perfumery. FOL can be synthesized in the liquid or vapor phase. Typical hydrogenation of furfural with hydrogen under high pressure to produce FOL is concerned with safety issues. Catalytic transfer hydrogenation (CTH) of furfural with hydrogen donors (methanol, ethanol, *n*-propanol, *i*-propanol, *n*-butanol, or *i*-butanol) with the assistance of Lewis acid sites has been reported as a feasible alternative. Homogeneous catalysts have been used for the reaction with issues related to corrosiveness, and complicated separation between reactants and products. Thus, heterogeneous catalysts have been used widely employed systems with simplified catalyst recovery after the reaction and improved stability [13,14]. Hydrogenation of furfural was catalyzed by metal oxides (Fe_3O_4, TiO_2, and NiO) on

* Corresponding author at: Departamento de Química Orgánica Universidad de Córdoba, Edificio Marie Curie (C 3), Campus de Rabanales, Ctra Nnal IV-A, Km 396, E14014 Córdoba, Spain.
E-mail address: rafael.luque@uco.es (R. Luque).

https://doi.org/10.1016/j.catcom.2023.106649
Received 5 December 2022; Received in revised form 16 March 2023; Accepted 19 March 2023
Available online 21 March 2023

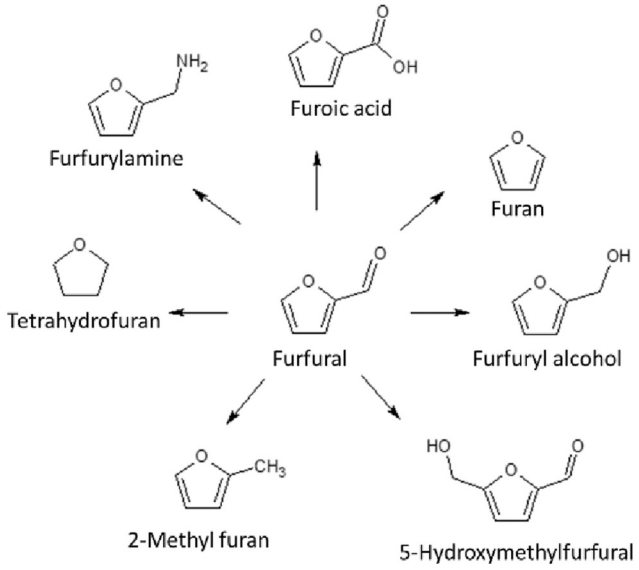

Scheme 1. Furfural conversion into important chemical compounds [7].

support, alumina or Metal-organic frameworks (MOFs).

MOFs are known as multifunctional materials used as catalysts, gas or liquid storage, sensing, separation and other applications because of their high surface area, porosity, tunable pore size, and thermal stability [15,16]. >20,000 different structures of MOFs are reported nowadays including structures such as UiO-66, UiO-67, MIL-100, ZIF-67, ZIF-8, and HKUST-1. They are formed by metal atoms as nodes and ligands synthesized by solvothermal, mechanochemistry or electrochemical methods [17,18]. MIL-101(Fe), and MIL-125(Ti) are well-known MOFs used in catalytic reactions and absorbents in wastewater. Moreover, they are the most surrogate materials of MIL-n series (MIL = *Matériaux de* l'Institut Lavoisier) [19]. Some previous works reported that metal oxides could catalyze furfural hydrogenation due to their Lewis acid sites that worked on the reaction. Moreover, metal oxides can proceed alkylation, reduction, condensation, cycloaddition, transesterification, dehydrogenation, and other chemical reactions efficiently with variety of reaction conditions. MOFs calcination can convert metal ions to metal oxides that are well-dispersed on carbon material to prevent aggregation. This could help improvement of catalytic activity and reduce metal leaching after reaction. Mhadmhan et al. studied evaluated the catalytic activity of synthesized Fe/Al-SBA-15, 53MOF/Al-SBA-15, 88MOF/Al-SBA-15 and 101MOF/Al-SBA-15 catalysts with different Fe sources in the N-alkylation of aniline with benzyl alcohol [20]. These catalysts were mesoporous materials with high surface areas. The acidity of catalysts was comparably improved with respect to Al-SBA-15 which increased aniline conversion. The use of MOFs as seeds increased Fe oxide nanoparticles dispersion on the support surface. 53MOF/Al-SBA-15 gave the best catalytic activity which indicated that the use of MOFs as seeds was more effective than the use of $FeCl_3$ (Fe/Al-SBA-15 catalyst). 53MOF/Al-SBA-15 could be reused due to its stability as mechanochemically synthesized catalyst [20].

Pirmoradi et al. reported about furfural hydrogenation over Pd-TiO_2 supported on activated carbon catalyst. [21] Metal sites and TiO_2 acted as active sites for the reaction. The reaction occurred through a continuous reactor system with H_2 gas at 180 °C and 2.1 MPa. Products were 2-MF, tetrahydrofurfuryl alcohol (THFA), 5-hydroxy-2-pentanone (5H2P), and FOL as an intermediate. The fractional conversion of furfural was about 0.50 mol/mol within 0.011 h with FOL as the main product. 5H2P selectivity and furfural conversion were increasing over time. Moreover, mechanism and mass transfer analysis were studied in this work.

Li et al investigated furfural hydrogenation over Fe_3O_4@C magnetic catalysts [22]. The catalyst was synthesized by a solvothermal process forming Fe_3O_4 and graphitic carbon from glucose. Increasing glucose and Fe_3O_4 ratio caused thicker the coated carbon shell of the catalyst. Fe_3O_4@C catalyzed furfural hydrogenation with isopropanol as a hydrogen donor and obtained FOL as the main product. Isopropanol has been reported as optimum H_2 donor compared to other alcohols (methanol, ethanol, n-propanol, n-butanol, and *i*-butanol) as it is a secondary alcohol. The optimum conditions were 473 K, within 4 h, and 0.05 g of catalyst and this provided 93.6% of FF conversion and 98.9% of FOL selectivity. Moreover, the catalyst could be recycled efficiently.

Last but least, dealing with the sustainability of a process also requires its scalability at industrial level. In this sense, continuous flow offers significant advantages with respect to batch systems including a precise control of mass and heat transfer, a fine residence time control, safer processes, continuous production and an easier scalability [23].

In this work, the possibility to obtain transition-metal-based oxide catalysts usable in a continuous flow system for the conversion of furfural with high performances was explored. For this purpose, C-MIL-101(Fe) and C-MIL-125(Ti) were synthesized by calcination of the parent MOFs obtained by hydrothermal synthesis. They were characterized by XRD, FT-IR, BET, XPS, TEM, and pyridine (PY), and 2,6-dimethyl pyridine (DMPY) pulse chromatography titration and tested with furfural hydrogenation reaction through a flow reactor system. Results were compared with previous works of furfural hydrogenation using a variety of catalysts including our recent work on similar Ti—Fe mixed oxide systems obtained from MOFs [24]. The calcined MIL-101 (Fe) and calcined MIL-125(Ti) were interesting due to the well-dispersed iron and titanium oxides as the active sites on the catalysts. Moreover, these metals (Fe and Ti) are not as expensive as Pd or Au which were selected to catalyze in other work of furfural hydrogenation.

2. Experimental

2.1. Catalyst preparation

MIL-101(Fe) was synthesized using 1.461 g of Iron (III) chloride hexahydrate ($FeCl_3{\cdot}6H_2O$) and 0.427 g of terephthalic acid. These chemicals were dissolved in 30 mL dimethylformamide (DMF) and stirred for 1 h at room temperature. Then, the mixture was transferred into autoclave and placed in the oven at 120 °C for 20 h. The solid was cool down, filtrated, and rinsed with DMF and ethanol, respectively, for few times. The obtained MIL-101(Fe) was dried in the vacuum oven for 70 °C overnight.

MIL-125(Ti) was prepared using 0.6 mL of titanium(IV) isopropoxide and 0.498 g of terephthalic acid. The chemicals were dissolved in DMF (15 mL) and methanol (2 mL) solvents stirring for 20 min at room temperature. The mixture was added to the autoclave and heated to 150 °C for 20 h. Then, the precipitate was cool down, filtrated and rinsed with DI water and ethanol for few times. After that, the white solid was dried at 80 °C for 2 h. The DMF in the white solid was removed by calcination at 200 °C for 10 h. Finally, MIL-125(Ti) was obtained.

Both MOFs were calcined to render C-MIL-101(Fe) and C-MIL-125 (Ti) (iron oxides and titanium oxides) used as catalysts. MIL-101(Fe) was calcined at 380 °C for 1 h under N_2 atmosphere while the MIL-125(Ti) was heated at 400 °C for 3 h under N_2 atmosphere for the calcination. All MOF and calcined MOFs were characterized by XRD, FT-IR, BET, XPS, and pyridine (PY), and 2,6-dimethyl pyridine (DMPY) pulse chromatography titration.

2.2. Catalyst characterization

Nitrogen physisorption isotherms were determined at 77 K by using the micromeritics automatic analyzer ASAP 2000 to study the textural properties of the materials. Each sample was degassed at 130 °C overnight under vacuum (0.1 Pa). The specific surface areas were obtained by the linear determination of the Brunauer-Emmett-Telller (BET)

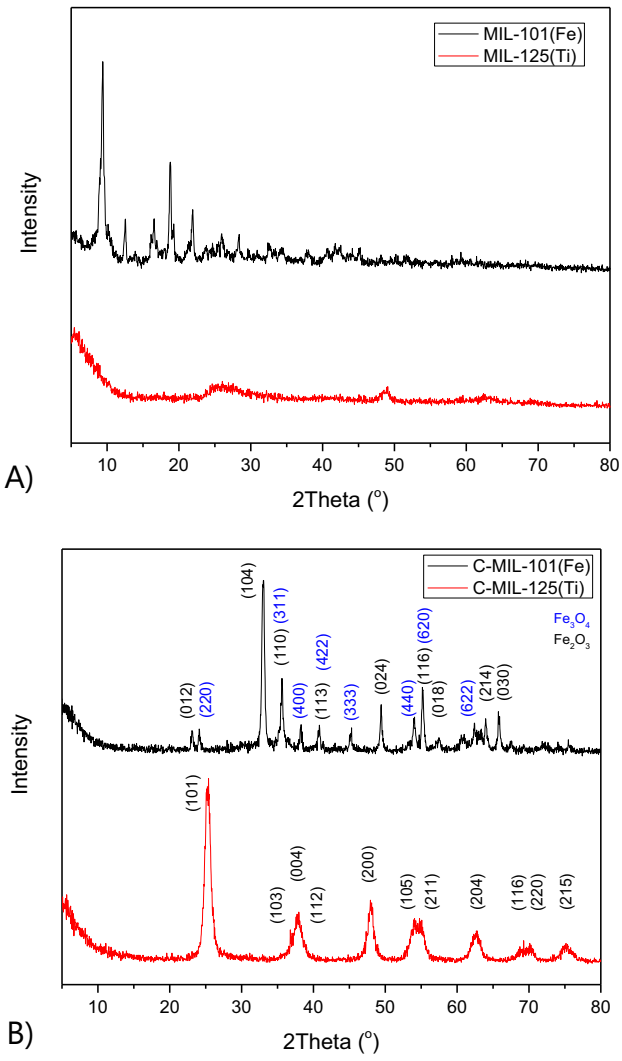

Fig. 1. XRD patterns of MIL-101(Fe) and MIL-125(Ti) (A) and XRD patterns of C-MIL-101(Fe) and C-MIL-125(Ti) (B).

equation.

Samples were analyzed by X-ray diffraction (XRD) with a Bruker D8-Advanced Diffractometer (40 kV, 40 mA) and Cu X-ray tube ($\lambda = 0.15$ A) (Bruker AXS, Karlsruhe, Germany). XRD patterns were measured in the range of 10°–80° (2Θ) to study crystallinity and structure of the solid materials. Materials were measured between 4000 and 400 cm^{-1} by A PerkinElmer spectrum 3 spectrophotometer and PIKE Technologies MIRacle™ Single Reflection ATR accessory for spectra IR.

XPS measurements were performed using an ultra-high vacuum (UHV) surface analysis system (Specst model, Berlin, Germany) at pressures $<10^{-10}$ mbar with a conventional XR-50 X-ray source (Specs, Mg-Ka, 1253.6 eV) in stop-and-go mode to reduce damage. Fe and Ti high-resolution spectra with pass energies of 25 and 10 eV and step sizes of 1 and 0.1 eV, respectively, were recorded at room temperature with a Phoibos 150-MCD energy analyzer (Phoibos, Berlin, Germany). Powdered samples were deposited on a sample holder with double-sided adhesive tape and evacuated overnight ($<10^{-6}$ Torr). The holder containing the degassed sample was transferred to the analysis chamber for XPS measurements. Binding energies were referenced to the adventitious carbon C1s line at 284.6 eV, and deconvolution curves were obtained using the manufacturer-supplied software Casa XPS.

Surface acid properties of the materials were analyzed by pyridine (PY), and 2,6-dimethyl pyridine (DMPY) pulse chromatography titration. The pulses were carried out using a microinjector in the catalytic bed from a cyclohexane solution of the titrant (0.989 M in PY and 0.956 M in DMPY). The catalyst was fixed inside a stainless-steel tubular microreactor with Pyrex glass wool stoppers and standardized at each titration at 200 °C in the nitrogen flow (99.999% purity). The gas chromatography with a flame ionization detector (FID) was used to analyze the injected base left from the catalyst to calculate the amount of acid sites on the catalyst surface.

2.3. Catalytic studies

The catalysts were tested in the hydrogenation of furfural (2 mmol) with 2-propanol (10 mL) under 200 °C and 20 bar with reactants flow rate of 0.2 mL/min for 2 h using a Phoenix flow reactor. 0.1 g packed catalyst (30 mm long ThalesNano CatCart) was employed. Products were collected every 15 min and analyzed by Gas Chromatography – Mass Spectrometry (GC–MS) and Gas Chromatography with Flame Ionization Detector (GC-FID).

3. Results and discussion

MOFs and the calcined MOFs were characterized by X-ray diffraction (XRD). XRD patterns of MIL-101(Fe) and MIL-125(Ti) have been included in Fig. 1a. The results show that MIL-101(Fe) had diffraction patterns at 9.42°, 9.66°, and 18.88° supporting a crystalline MIL-101 (Fe) formation [25,26]. Comparably, MIL-125 shows an amorphous material with broad peaks before 10°, around 25° and 50°. Even if not crystalline, this MOF will transform in anatase and rutile TiO_2 upon calcination.

Fig. 1b shows XRD patterns of calcined MOFs. C-MIL-125(Ti) illustrated diffraction peaks at 2Θ = 25.8°, 38.7°, 48.3°, 54.4°, 55.4°, 63°, 69.5°, and 75°, representing the typical anatase phase (TiO_2). Moreover, there were less intense diffraction patterns at 27.1° and 36.1° ascribed to the rutile phase in the C-MIL-125(Ti). These indicated that MIL-125(Ti) had changed to anatase and rutile TiO_2 after calcination [27]. XRD diffraction of C-MIL-101(Fe) showed 2Θ lines at 24.12°, 33.12°, 35.61°, 40.88°, 49.51°, 54.22°, 57.63°, 62.45°, and 64.11° ascribed to hematite Fe_2O_3 phase [28]. In addition, there were weak diffraction patterns of a different iron oxide species after MIL-101(Fe) calcination. Appearing at 2Θ values of 30.1°, 35.4°, 43.1°, 53.4°, 56.9°, and 62.3°.

FT-IR patterns of MOFs are shown in Fig. 2. There were apparent peaks in the region of 1600–1400 cm^{-1} representing asymmetric and symmetric O-C-O bonds of terephthalic acid ligands of MIL-101(Fe) in Fig. 2a. Moreover, peaks at 590 and 790 cm^{-1} belonged to Fe—O vibration and C—H bending vibration of benzene of MIL-101(Fe), respectively [17,19]. In Fig. 2b, strong bands around 1650 and 1400 cm^{-1} ascribed to vibrational stretching of the carboxylate ($-COO^-$) group of the ligands of MIL-125(Ti). In addition, there were peaks between 500 and 800 cm^{-1} assigned to O-Ti-O vibrations [29].

Table 1 shows textural and porosity results of calcined MOFs (C-MIL-101(Fe) and C–MIL-125(Ti)) determined by N_2 adsorption/desorption isotherms. C-MIL-125(Ti) had the largest BET surface area, pore diameter, and mesopore volume compared to C-MIL-101(Fe). Moreover, all calcined MOFs showed a type IV isotherm with an H3 hysteresis loop that demonstrated mesopore materials with wedge-shaped pores as shown in Fig. 3.

PY and DMPY pulse chromatography titration experiments were subsequently performed to estimate the acid properties of the catalysts. This characterization pointed to the presence of Lewis and Brönsted acid sites on the catalysts when DMPY is selectively adsorbed on only Brönsted acid sites while PY is adsorbed on both of Lewis and Brönsted acid sites. Therefore, the difference between PY and DMPY adsorption could indicate Lewis acid sites on the catalysts. Table 1 showed that the biggest difference between DMPY and PY belonged to C-MIL-125(Ti), demonstrating that C-MIL-125(Ti) had the largest amount of Lewis acid sites. On the contrary, C-MIL-101(Fe) had a small amount of Lewis acid sites but a higher amount of Brönsted acid sites.

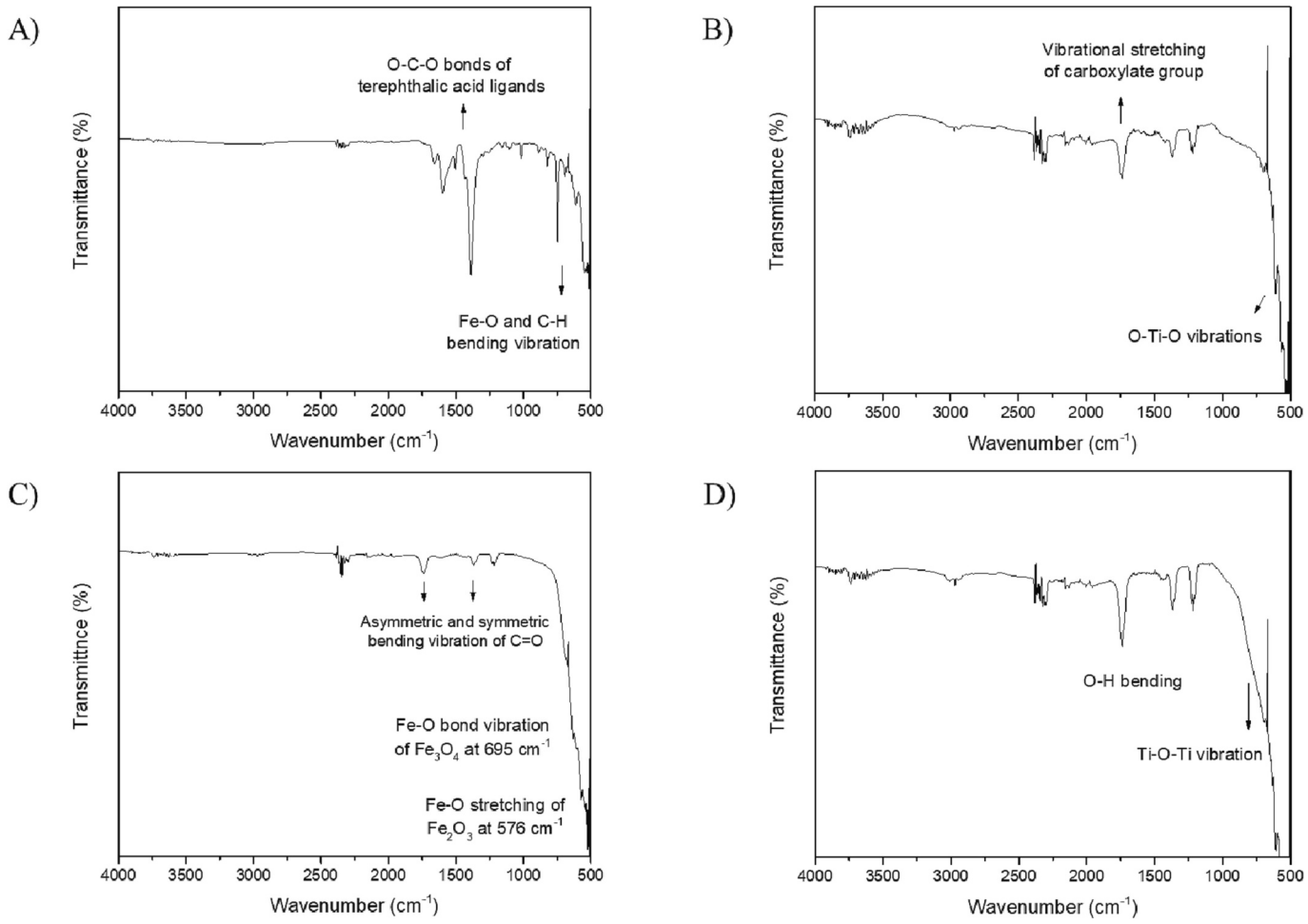

Fig. 2. FT-IR patterns of MIL-101(Fe) (A), MIL-125(Ti) (B), calcined MIL-101(Fe) (C) and calcined MIL-125(Ti) (D).

Table 1
Textural properties obtained from N_2 sorption experiments and acid properties achieved from PY and DMPY pulse chromatography titration of calcined MOFs.

Catalysts	BET surface area (m^2/g)	Mesopore volume (cm^3/g)	Pore diameter (Å)	PY (μmol/g)	DMPY (μmol/g)
C-MIL-101 (Fe)	119	0.23	38.4	69	62
C-MIL-125 (Ti)	122	0.28	83.0	119	25

Fig. 4 shows XPS spectra of C-MIL-101(Fe) and C-MIL-125(Ti). The calibration of binding energies was reported respect to the main C 1 s peak set at 284.6 eV. For C-MIL-101(Fe) (Fig. 5A), the spectrum showed two contributions in the carbon region at 284.5 eV and 288.1 eV, attributable to sp^2 C═C and C═O respectively. In the O 1 s region, the main peak was deconvoluted in three contributions at 530.4 eV, 531.7 eV and 533.3 eV attributable to Fe—O lattice oxygen, Fe-OH (or defective oxide) that is the main peak, and C═O, respectively [30,31]. In the Fe 2p region, there were 2 peaks of Fe 2p at 709.9 eV with a classical broadening few eV away for paramagnetic oxides [32] and one at 723.9 eV which corresponded to Fe $2p_{3/2}$ and Fe $2p_{1/2}$ spin orbitals, respectively, attributable to Fe^{3+} species.

The spectrum of C-MIL-125(Ti) (Fig. 4B) showed three contributions to the signal in the C 1 s region. Two of them are attributable again to C═C and C═O species (respectively at 284.5 eV and 288.5 eV) but a third contribution was present in this sample at 285.7 attributable to

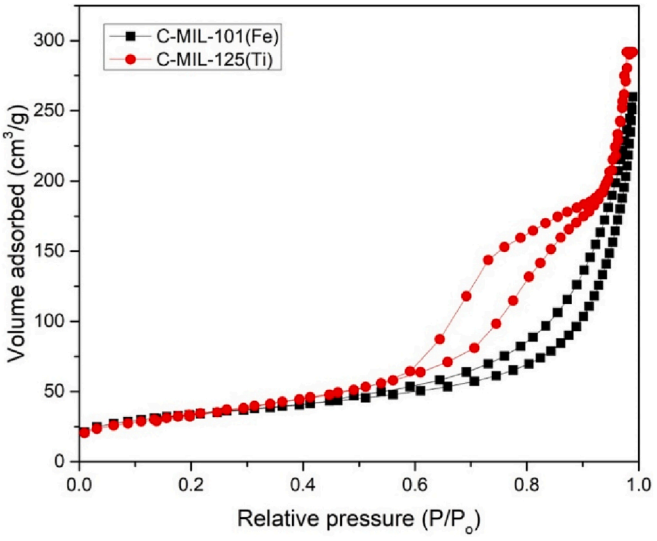

Fig. 3. N_2 adsorption/desorption isotherms of calcined MOFs (C-MIL-101(Fe) and C-MIL-125(Ti)).

C—O single bond, indicating the possible presence of -C-OH moieties [33,34]. The O 1 s region could be deconvoluted into three bands correspond to Ti—O lattice species (larger contribution, 529.8 eV), Ti-OH (531.3 eV) and C═O species [35], comparably different to Fe-

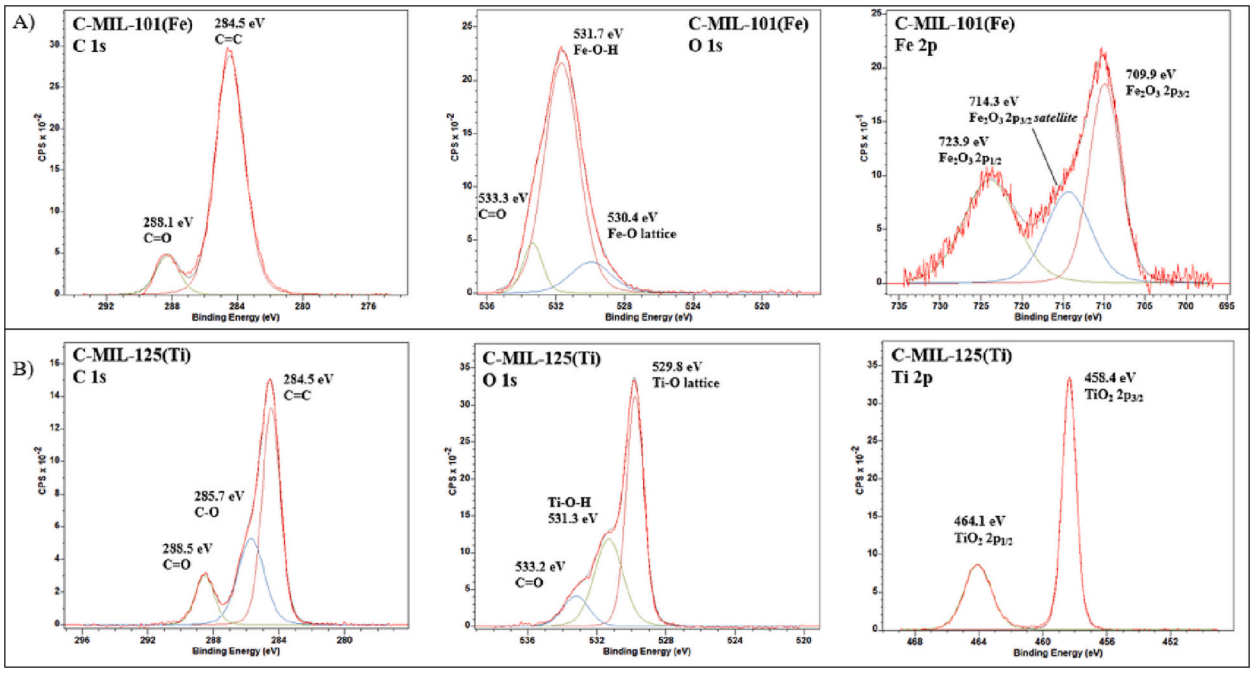

Fig. 4. XPS analysis of calcined MOFs A) C-MIL-101(Fe) and B) C-MIL-125(Ti)).

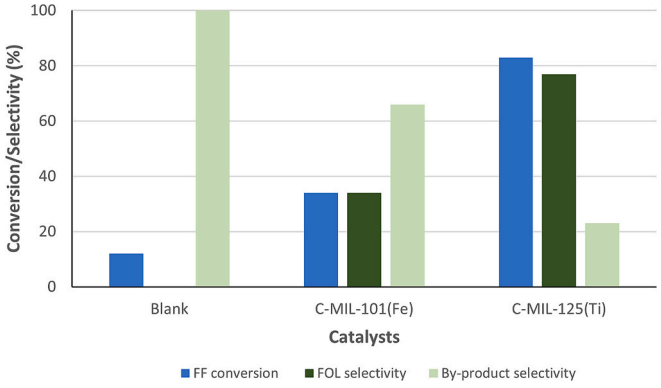

Fig. 5. Catalytic activity of furfural hydrogenation with 2-propanol over calcined MOFs with Phoenix flow reactor. (Reaction conditions: 200 °C, 20 bar, reactants flow rate of 0.2 mL/min, and reaction time = 2 h).

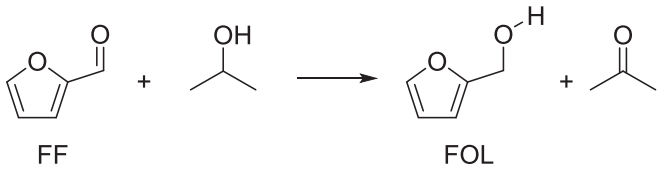

Scheme 2. Furfural hydrogenation to obtain FOL.

containing materials in which the largest contribution was due to Fe-OH species. The presence of mainly non-protonated oxygen in the TiO_2 of C-MIL-125(Ti) can be the reason why the contribution of Lewis acid sites is higher in this material as compared to that of C-MIL-101(Fe). In the Ti 2p region, peaks of Ti 2p were present at 464.1 and 458.4 eV, correlated to Ti $2p_{1/2}$ and Ti $2p_{3/2}$ of Ti^{4+} (typical of TiO_2).

Li, et al. studied the optimum conditions for furfural hydrogenation (Scheme 2) [22]. The type of alcohol (H_2 donors) plays an important role in the reaction. Interestingly, 2-propanol had low reduction ability. Moreover, the H atom at the α-C position of 2-propanol could be easily activated and lead to improved reaction yields. High FF conversion was achieved when the temperature was increased from 160 to 200 °C.

Table 2
Comparative catalytic activity of furfural hydrogenation using various catalysts.

Catalysts	Conditions	FF conversion (%)	FOL selectivity (%)	References
Fe_3O_4/C	Furfural, 2-propanol, batch reactor, 200 °C, 20 bar, 4 h	76.4	98.5	[36]
5% Pd/TiO_2 5% Ru/TiO_2 1%Ru-4%Pd/TiO_2	Furfural, H_2, batch reactor, 200 °C, 20 bar, and 4 h	65.4 8.2 39.3	28.6 100 45.3	[37]
TiO_2-Fe_2O_3/C	Furfural, 2-propanol, formic acid (Furfural/formic acid 2:1 ratio) flow reactor, 200 °C, 30 bar, 0.1 mL/min flow rate, 1.5 h, 0.25 g catalyst	70	>99	[24]
C-MIL-125 (Ti)	Furfural, 2-propanol, flow reactor, 200 °C, 20 bar, 0.2 mL/min flow rate, 2 h, 0.1 g catalyst	83	77	This work

Calcined MOFs were tested in furfural hydrogenation using 2-propanol as an H_2 donor to obtain furfuryl alcohol (FOL), with catalyst performance being depicted in Fig. 5. Blank runs (without catalyst) provided very low FF conversion with only furfuryl diacetate (FLDA) as major product. On the other hand, the reaction with catalysts could produce FOL, for which C-MIL-125(Ti) had the highest FF conversion (83%) and 77% FOL selectivity. FLDA, 2-furanmethanol acetate (2-FMA) and 3-butene-2-one, 4-(2-furanyl)-(3-BOF) were detected by-products during furfural hydrogenation over C-MIL-125(Ti). Unexpectedly, the reaction with C-MIL-101(Fe) provided a comparably low FF conversion (34%). This result showed that the textural and surface

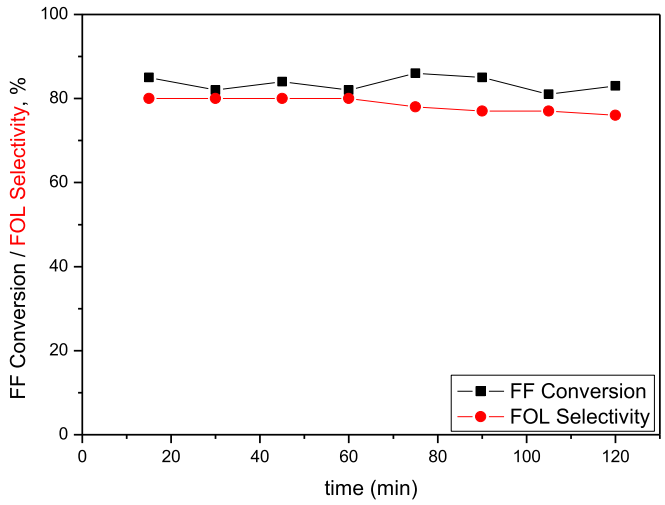

Fig. 6. FF Conversion and FOL Selectivity vs. time using C-MIL125(Ti) catalyst. (Reaction conditions: 200 °C, 20 bar, reactants flow rate of 0.2 mL/min, and reaction time = 2 h).

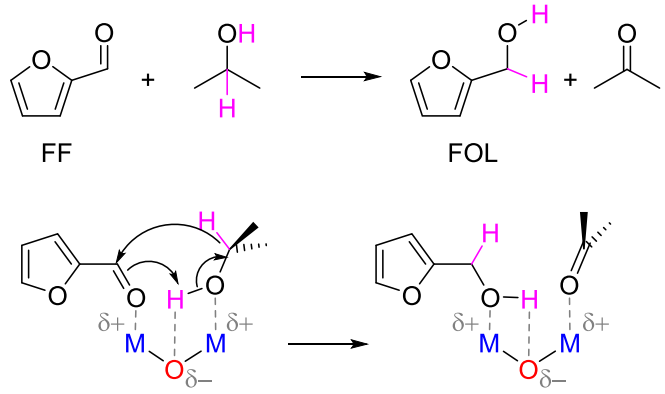

Scheme 3. Catalytic transfer hydrogenation (CTH) of furfural to furfuryl alcohol over catalyst (calcined MOFs).

properties of catalysts influenced FF conversion and FOL selectivity.

Table 2 shows the catalytic activity of furfural hydrogenation with 2-propanol over Fe_3O_4/C catalyst [36] under autoclave conditions provided 76.4% FF conversion. Fe_3O_4/C catalyst was prepared via Fe MOF calcination. The well dispersed metal oxides on the catalyst could help to provide high FOL selectivity. On the other hand, furfural hydrogenation over 5% Pd/TiO_2 (without alcohol as H_2 donor) provided 65.4% FF conversion with low FOL selectivity. 5% Ru/TiO_2 was reported to lead to complete FOL selectivity at very low conversion (ca. 8%). Bimetallic 1% Ru-4%Pd/TiO_2 was prepared to improve FOL selectivity and conversion but the use of molecular hydrogen might cause safety issues during the reaction. In this work, C-MIL-125(Ti) offered a remarkably high FF conversion (83%) with high FOL selectivity under simpler reaction conditions as compared to our recently reported combined Ti—Fe oxides from MOFs (requiring double catalyst amount and the addition of formic acid to react 70% furfural conversion) [24].

FF conversion profile FF and FOL selectivity vs time is shown in Fig. 6, remaining stable with time-on-stream which pointed to a good stability of the catalytic system under the investigated reaction conditions.

Catalytic transfer hydrogenation (CTH) is used to explain the mechanism of furfural hydrogenation with alcohol as an H_2 source on the Lewis acid sites of iron or titanium oxides as well-known and previously reported reaction mechanism, Scheme 3 [38,39].

4. Conclusions

Metal oxides were directly obtained upon calcination of Ti and Fe-containing MOFs. C-MIL-125(Ti) performed better than C-MIL-101(Fe) in furfural hydrogenation to FOL. C-MIL-125(Ti) provided 83% furfural conversion with 77% FOL selectivity due to the presence of larger amount of Lewis acid sites and optimum porosity. Furfural conversion was also achieved in high yields, in a scalable continuous flow system, using simple, highly stable and active transition metal based oxide catalysts (Ti and Fe).

Credit author statement

Janejira Ratthiwal: investigation, experiments, writing first draft.
Noelia Lazaro: investigation, experiments.
Antonio Pineda: analysis, validation, investigation.
Roberto Esposito: supervision, validation, writing and editing-revised draft.
Zeid A. ALOthman: validation, writing and editing-first draft.
Prasert Reubroycharoen: supervision, writing and editing-first draft.
Rafael Luque: conceptualization, supervision, resources, validation, writing and editing-first draft and revised final draft.

Declaration of Competing Interest

The authors declare that they have no known competing financial interests or personal relationships that could have appeared to influence the work reported in this paper.

Data availability

Data will be made available on request.

Acknowledgments

Rafael Luque gratefully acknowledges MINECO for the concession of project PID2019-109953GB-I00, co-financed with FEDER funds. This work was supported by the Distinguished Scientist Fellowship Program (DSFP) at King Saud University, Riyadh, Saudi Arabia. All reviewers of this manuscript (especially reviewer 3) are gratefully acknowledged with many thanks for their useful suggestions, careful consideration and patience during the revisions of this manuscript.

References

[1] J.C. Serrano-Ruiz, J.M. Campelo, M. Francavilla, A.A. Romero, R. Luque, C. Menéndez-Vázquez, A.B. García, E.J. García-Suárez, Efficient microwave-assisted production of furfural from C5 sugars in aqueous media catalysed by Brönsted acidic ionic liquids, Catal, Sci. Technol. 2 (2012) 1828–1832.
[2] L. Ji, P. Li, F. Lei, X. Song, J. Jiang, K. Wang, Coproduction of furfural, phenolated lignin and fermentable sugars from bamboo with one-pot fractionation using phenol-acidic 1,4-Dioxane, Energies 13 (2020) 5294.
[3] T. Yang, W. Li, M. Su, Y. Liu, M. Liu, Production of furfural from xylose catalyzed by a novel calcium gluconate derived carbon solid acid in 1,4-dioxane, New J. Chem. 44 (2020) 7968–7975.
[4] A. Jaswal, P.P. Singh, T. Mondal, Furfural – a versatile, biomass-derived platform chemical for the production of renewable chemicals, Green Chem. 24 (2022) 510–551.
[5] D.S. Naidu, S.P. Hlangothi, M.J. John, Bio-based products from xylan: a review, Carbohydr. Polym. 179 (2018) 28–41.
[6] W. Hui, Y. Zhou, Y. Dong, Z.-J. Cao, F.-Q. He, M.-Z. Cai, D.-J. Tao, Efficient hydrolysis of hemicellulose to furfural by novel superacid SO4H-functionalized ionic liquids, Green Energy & Environment 4 (2019) 49–55.
[7] R. Mariscal, P. Maireles-Torres, M. Ojeda, I. Sádaba, M. López Granados, Furfural: a renewable and versatile platform molecule for the synthesis of chemicals and fuels, Energy Environ. Sci. 9 (2016) 1144–1189.
[8] T. Tongtummachat, N. Akkarawatkhoosith, A. Kaewchada, A. Jaree, Conversion of glucose to 5-hydroxymethylfurfural in a microreactor, Frontiers in Chemistry 7 (2020).
[9] Y. Qu, Y. Zhao, S. Xiong, C. Wang, S. Wang, L. Zhu, L. Ma, Conversion of glucose into 5-hydroxymethylfurfural and levulinic acid catalyzed by SO42–/ZrO2 in a biphasic solvent system, Energy Fuel 34 (2020) 11041–11049.

[10] M. Melchiorre, D. Lentini, M.E. Cucciolito, F. Taddeo, M. Hmoudah, M. Di Serio, F. Ruffo, V. Russo, R. Esposito, Sustainable ketalization of glycerol with ethyl levulinate catalyzed by the Iron(III)-based metal-organic framework MIL-88A, Molecules 27 (2022) 7229.
[11] X. Chen, L. Zhang, B. Zhang, X. Guo, X. Mu, Highly selective hydrogenation of furfural to furfuryl alcohol over Pt nanoparticles supported on g-C3N4 nanosheets catalysts in water, Sci. Rep. 6 (2016) 28558.
[12] A. Sreenavya, V. Ganesh, N.J. Venkatesha, A. Sakthivel, Hydrogenation of biomass derived furfural using Ru-Ni-Mg–Al-hydrotalcite material, Biomass Conversion and Biorefinery (2022), https://doi.org/10.1007/s13399-022-02641-8.
[13] M.S. Gyngazova, L. Grazia, A. Lolli, G. Innocenti, T. Tabanelli, M. Mella, S. Albonetti, F. Cavani, Mechanistic insights into the catalytic transfer hydrogenation of furfural with methanol and alkaline earth oxides, J. Catal. 372 (2019) 61–73.
[14] Z. An, J. Li, Recent advances in the catalytic transfer hydrogenation of furfural to furfuryl alcohol over heterogeneous catalysts, Green Chem. 24 (2022) 1780–1808.
[15] J. Li, L. Wang, Y. Liu, P. Zeng, Y. Wang, Y. Zhang, Removal of berberine from wastewater by MIL-101(Fe): performance and mechanism, ACS Omega 5 (2020) 27962–27971.
[16] Z. Liu, W. He, Q. Zhang, H. Shapour, M.F. Bakhtari, Preparation of a GO/MIL-101 (Fe) composite for the removal of methyl orange from aqueous solution, ACS Omega 6 (2021) 4597–4608.
[17] A.D.S. Barbosa, D. Julião, D.M. Fernandes, A.F. Peixoto, C. Freire, B. de Castro, C. M. Granadeiro, S.S. Balula, L. Cunha-Silva, Catalytic performance and electrochemical behaviour of metal–organic frameworks: MIL-101(Fe) versus NH2-MIL-101(Fe), Polyhedron 127 (2017) 464–470.
[18] M.H. Yap, K.L. Fow, G.Z. Chen, Synthesis and applications of MOF-derived porous nanostructures, Green Energy & Environment 2 (2017) 218–245.
[19] C. Gecgel, U.B. Simsek, B. Gozmen, M. Turabik, Comparison of MIL-101(Fe) and amine-functionalized MIL-101(Fe) as photocatalysts for the removal of imidacloprid in aqueous solution, J. Iran. Chem. Soc. 16 (2019) 1735–1748.
[20] S. Mhadmhan, M.D. Marquez-Medina, A.A. Romero, P. Reubroycharoen, R. Luque, Fe-containing MOFs as seeds for the preparation of highly active Fe/Al-SBA-15 catalysts in the N-alkylation of aniline, Molecules 24 (15) (2019) 2695.
[21] M. Pirmoradi, J.R. Kastner, A kinetic model of multi-step furfural hydrogenation over a Pd-TiO2 supported activated carbon catalyst, Chem. Eng. J. 414 (2021), 128693.
[22] F. Li, S. Jiang, J. Huang, Y. Wang, S. Lu, C. Li, Catalytic transfer hydrogenation of furfural to furfuryl alcohol over a magnetic Fe3O4@C catalyst, New J. Chem. 44 (2020) 478–486.
[23] D. Dallinger, C.O. Kappe, Why flow means green – evaluating the merits of continuous processing in the context of sustainability, Curr. Opin. Green Sustain. Chem. 7 (2017) 6–12.
[24] M. Ronda-Leal, S.M. Osman, H. Won Jang, M. Shokouhimehr, A.A. Romero, R. Luque, Selective hydrogenation of furfural using TiO2-Fe2O3/C from Ti-Fe-MOFs as sacrificial template: microwave vs continuous flow experiments, Fuel 333 (2023), 126221.
[25] D. Yan, H. Hu, N. Gao, J. Ye, H. Ou, Fabrication of carbon nanotube functionalized MIL-101(Fe) for enhanced visible-light photocatalysis of ciprofloxacin in aqueous solution, Appl. Surf. Sci. 498 (2019), 143836.
[26] Y. Huang, H. Lin, Y. Zhang, Synthesis of MIL-101(Fe)/SiO2 composites with improved catalytic activity for reduction of nitroaromatic compounds, J. Solid State Chem. 283 (2020), 121150.
[27] M. Alfè, V. Gargiulo, M. Amati, V.-A. Maraloiu, P. Maddalena, S. Lettieri, Mesoporous TiO2 from metal-organic frameworks for photoluminescence-based optical sensing of oxygen, Catalysts 11 (7) (2021) 795.
[28] L.M. Cursaru, R.M. Piticescu, D.V. Dragut, I.A. Tudor, V. Kuncser, N. Iacob, F. Stoiciu, The influence of synthesis parameters on structural and magnetic properties of iron oxide nanomaterials, Nanomaterials 10 (1) (2020) 85.
[29] Y. Zhao, W. Cai, J. Chen, Y. Miao, Y. Bu, A highly efficient composite catalyst constructed from NH2-MIL-125(Ti) and reduced graphene oxide for CO2 photoreduction, Frontiers in Chemistry 7 (2019).
[30] M.C. Biesinger, B.P. Payne, A.P. Grosvenor, L.W.M. Lau, A.R. Gerson, R.S.C. Smart, Resolving surface chemical states in XPS analysis of first row transition metals, oxides and hydroxides: Cr, Mn, Fe, Co and Ni, Appl. Surf. Sci. 257 (2011) 2717–2730.
[31] J.-C. Wang, J. Ren, H.-C. Yao, L. Zhang, J.-S. Wang, S.-Q. Zang, L.-F. Han, Z.-J. Li, Synergistic photocatalysis of Cr(VI) reduction and 4-Chlorophenol degradation over hydroxylated α-Fe2O3 under visible light irradiation, J. Hazard. Mater. 311 (2016) 11–19.
[32] E. Paparazzo, On the quantitative XPS analysis of Fe2O3 and Fe1−xO oxides, J. Electron Spectrosc. Relat. Phenom. 154 (2006) 38–40.
[33] R. Yan, H. Wu, Q. Zheng, J. Wang, J. Huang, K. Ding, Q. Guo, J. Wang, Graphene quantum dots cut from graphene flakes: high electrocatalytic activity for oxygen reduction and low cytotoxicity, RSC Adv. 4 (2014) 23097–23106.
[34] D. Rodríguez-Padrón, M. Algarra, L.A.C. Tarelho, J. Frade, A. Franco, G. de Miguel, J. Jiménez, E. Rodríguez-Castellón, R. Luque, Catalyzed microwave-assisted preparation of carbon quantum dots from lignocellulosic residues, ACS Sustain. Chem. Eng. 6 (2018) 7200–7205.
[35] M.C. Biesinger, L.W.M. Lau, A.R. Gerson, R.S.C. Smart, Resolving surface chemical states in XPS analysis of first row transition metals, oxides and hydroxides: Sc, Ti, V, Cu and Zn, Appl. Surf. Sci. 257 (2010) 887–898.
[36] S. Jiang, J. Huang, Y. Wang, S. Lu, P. Li, C. Li, F. Li, Metal–organic frameworks derived magnetic Fe3O4/C for catalytic transfer hydrogenation of furfural to furfuryl alcohol, J. Chem. Technol. Biotechnol. 96 (2021) 639–649.
[37] O.F. Aldosari, S. Iqbal, P.J. Miedziak, G.L. Brett, D.R. Jones, X. Liu, J.K. Edwards, D.J. Morgan, D.K. Knight, G.J. Hutchings, Pd–Ru/TiO2 catalyst – an active and selective catalyst for furfural hydrogenation, Catal. Sci. Technol. 6 (2016) 234–242.
[38] S. Srivastava, G.C. Jadeja, J. Parikh, Copper-cobalt catalyzed liquid phase hydrogenation of furfural to 2-methylfuran: an optimization, kinetics and reaction mechanism study, Chem. Eng. Res. Des. 132 (2018) 313–324.
[39] A. Shivhare, A. Kumar, R. Srivastava, An account of the catalytic transfer hydrogenation and hydrogenolysis of carbohydrate-derived renewable platform chemicals over non-precious heterogeneous metal catalysts, ChemCatChem 13 (2021) 59–80.